

676

学位論文

**Integrated Analysis of DNA Methylation and Mutations
in Esophageal Squamous Cell Carcinoma.**

香川大学大学院医学系研究科

機能構築医学 専攻

岸野 貴賢

Integrated Analysis of DNA Methylation and Mutations in Esophageal Squamous Cell Carcinoma

Takayoshi Kishino,^{1,2,3} Tooru Niwa,¹ Satoshi Yamashita,¹ Takamasa Takahashi,^{1,2} Hidetsugu Nakazato,^{1,2} Takeshi Nakajima,⁴ Hiroyasu Igaki,² Yuji Tachimori,² Yasuyuki Suzuki,³ and Toshikazu Ushijima^{1*}

¹Division of Epigenomics, National Cancer Center Research Institute, Tokyo, Japan

²Division of Esophageal Surgery, National Cancer Center Hospital, Tokyo, Japan

³Department of Gastroenterological Surgery, Kagawa University, Kagawa, Japan

⁴Division of Endoscopy, National Cancer Center Hospital, Tokyo, Japan

The recent development of next-generation sequencing technology for extensive mutation analysis, and beadarray technology for genome-wide DNA methylation analysis has made it possible to obtain integrated pictures of genetic and epigenetic alterations, using the same cancer samples. In this study, we aimed to characterize such a picture in esophageal squamous cell carcinomas (ESCCs). Base substitutions of 55 cancer-related genes and copy number alterations (CNAs) of 28 cancer-related genes were analyzed by targeted sequencing. Forty-four of 57 ESCCs (77%) had 64 non-synonymous somatic mutations, and 24 ESCCs (42%) had 35 CNAs. A genome-wide DNA methylation analysis using an Infinium HumanMethylation450 BeadChip array showed that the CpG island methylator phenotype was unlikely to be present in ESCCs, a different situation from gastric and colon cancers. Regarding individual pathways affected in ESCCs, the WNT pathway was activated potentially by aberrant methylation of its negative regulators, such as *SFRP1*, *SFRP2*, *SFRP4*, *SFRP5*, *SOX17*, and *WIF1* (33%). The p53 pathway was inactivated by *TP53* mutations (70%), and potentially by aberrant methylation of its downstream genes. The cell cycle was deregulated by mutations of *CDKN2A* (9%), deletions of *CDKN2A* and *RB1* (32%), and by aberrant methylation of *CDKN2A* and *CHFR* (9%). In conclusion, ESCCs had unique methylation profiles different from gastric and colon cancers. The genes involved in the WNT pathway were affected mainly by epigenetic alterations, and those involved in the p53 pathway and cell cycle regulation were affected mainly by genetic alterations. © 2016 Wiley Periodicals, Inc.

Key words: epigenetics; DNA methylation; genetic alterations; esophageal squamous cell carcinoma (ESCC); cancer-related pathway

INTRODUCTION

Esophageal squamous cell carcinoma (ESCC) is one of the most malignant cancers worldwide, and a predominant histological type of esophageal cancer [1,2]. To understand ESCC development, many studies have been conducted showing that *TP53* is most frequently mutated (35–84%), and that other genes, such as *CDKN2A*, *CDKN2B*, *EGFR*, *NFE2L2*, *PIK3CA*, *MLH1*, and *BRAF*, are mutated with relatively low frequencies [3–7]. Recently, four comprehensive mutation analyses by whole-genome and whole-exome sequencing have been reported in ESCCs, and *ADAM29*, *AJUBA*, *ARID1A*, *FAM135B*, *FAT1*, *FAT2*, *FAT3*, *FAT4*, *KEAP1*, *KMT2D*, *NOTCH1*, *NOTCH2*, *NOTCH3*, and *ZNF750* were newly identified as mutated genes [8–11].

Epigenetic alterations, such as aberrant DNA methylation, are deeply involved in human cancer development [12–15]. Especially, aberrant DNA methylation of a CpG island (CGI) in a promoter region causes silencing of its downstream gene and is known as a major mechanism for inactivation of tumor-suppressor genes [16]. In ESCCs, *CDKN2A* has been reported to be methylated in 19–88% of cases [17–19], and its methylation is associated with metastatic and

invasive phenotypes of ESCCs [20]. Additional genes, such as *APC*, *CDH1*, *CDKN2B*, and *RASSF1*, have also been reported to be methylated in ESCCs [21–26].

In this study, we aimed to establish an integrated picture of genetic and epigenetic alterations in ESCCs taking advantage of two novel technologies. Next-generation sequencing (NGS) technology has enabled

Abbreviations: NGS, next-generation sequencing; ESCC, esophageal squamous cell carcinoma; CGI, CpG island; CNV, copy number variation; RRDR, relative reading depth to the reference; array-CGH, microarray-based comparative genomic hybridization; TSS, transcription start site; TSS200, 200-bp upstream region from a transcription start site; OS, overall survival; dCRT, definitive chemoradiotherapy; CIMP, CpG island methylator phenotype.

Grant sponsor: The Project for Development of Innovative Research on Cancer Therapeutics (P-DIRECT) from the Ministry of Education, Culture, Science, and Technology, Japan; Grant sponsor: Applied Research for Innovative Treatment of Cancer from the Ministry of Health, Labour and Welfare, Japan

*Correspondence to: Division of Epigenomics, National Cancer Center Research Institute, 5-1-1 Tsukiji, Chuo-ku, Tokyo 104-0045, Japan.

Received 15 April 2015; Revised 1 December 2015; Accepted 15 December 2015

DOI 10.1002/mc.22452

Published online 12 January 2016 in Wiley Online Library (wileyonlinelibrary.com).

CGH + SNP 4 × 180 K microarray (Agilent Technologies). The microarray was scanned with an Agilent G2565BA microarray scanner (Agilent Technologies), and the scanned data were processed using the Agilent CytoGenomics Software (Agilent Technologies). A relative copy number of a gene was obtained as two to the power of the mean log₂ ratio of all probes within the gene.

Analysis of Gene Expression by Oligonucleotide Microarray

Gene expression levels in normal esophageal mucosae and ESCC cell lines (KYSE30, KYSE50, KYSE220, and KYSE270) were analyzed using the GeneChip Human Genome U133 Plus 2.0 microarray (Affymetrix, Santa Clara, CA, USA), as described previously [32]. Genes with signal intensities of 250 or more were considered expressed genes.

Analysis of DNA Methylation

Analysis of DNA methylation was performed using an Infinium HumanMethylation450 BeadChip array, which covered 482,421 CpG and 3,091 non-CpG sites (Illumina, San Diego, CA), as described previously [33]. The methylation level of a CpG site was represented by a β value, which ranged from 0 (completely unmethylated) to 1 (completely methylated). A corrected β value was calculated using a measured beta value and the fraction of cancer cells in a sample [A corrected β value = the β value measured × 100 / (the fraction of cancer cells in the sample (%))] [28].

All the CpG sites were grouped into 193,531 genomic "segments", each of which was defined by its location against a transcription start site (TSS) and relative location against a CGI. Genomic segments were divided into 299,563 genomic "blocks" smaller than 500 bp, and 292,265 genomic blocks on autosomes were used for the analysis. The numbers of genomic segments and blocks in this study were different from those in our previous study [30]. This is because genomic segments and blocks with probes that failed to produce reliable β value in any samples were excluded in the previous study [30], but not in this study. A DNA methylation level of a genomic block was evaluated using the mean of corrected β values of the CpG sites within the genomic block, and the methylation status of the genomic block was classified into unmethylated (corrected β value < 0.4), partially methylated (0.4 ≤ corrected β value < 0.8), and heavily methylated (corrected β value ≥ 0.8).

Selection of Genes of Cancer-Related Pathways

Six cancer-related pathways (the WNT pathway, the AKT/mTOR pathway, the MAPK pathway, the p53 pathway, cell cycle regulation, and mismatch repair) were selected because these pathways have been repeatedly reported to be altered in ESCCs [9–11,34–37]. Genes involved in the six cancer-related pathways were selected from the Kyoto Encyclopedia of

Genes and Genomes Pathway Database (<http://www.genome.jp/kegg/>). Regarding the pathways activated in ESCCs, their negative regulators were selected. Regarding the pathways inactivated in ESCCs, their positive regulators and downstream effectors were selected. A total of 81 genes were selected for analyses of the six cancer-related pathways (Supplementary Table S4 and Figure S1). Among the 81 genes, 25 genes were analyzed for base substitutions, 67 genes for methylation silencing, and 11 genes for both (Supplementary Table S4 and Figure S1). For the analysis of methylation silencing, we used a CGI in a 200-bp upstream region from a transcription start site (TSS200) whenever probes were available in this region because DNA methylation of a CGI in a TSS200 is known to consistently silence its downstream gene [12,37–40] (Supplementary Table S5).

Western Blot Analysis

Proteins in total cell lysate (5 μ g) were separated by sodium dodecyl sulfate–polyacrylamide gel electrophoresis, and were transferred to a polyvinylidene difluoride membrane (Millipore, Billerica, MA). Phospho-p44/42 MAPK (ERK1/2) and p44/42 MAPK (ERK1/2) were detected using a rabbit polyclonal antibody against phospho-p44/42 MAPK (1:1,000; CST4370; Cell Signaling Technology, Danvers, MA), and a rabbit polyclonal antibody against p44/42 MAPK (1:1,000; CST4695; Cell Signaling Technology, Danvers, MA), respectively. Protein bands were visualized by enhanced chemiluminescence.

Clustering Analysis

Unsupervised hierarchical clustering analysis was performed using R 2.15 [R Core Team (2012) R: a language and environment for statistical computing. R Foundation for Statistical Computing, Vienna, Austria. ISBN 3-900051-07-0, URL <http://www.R-project.org/>] with the Heatplus package [Alexander Ploner (2011) Heatplus: Heatmaps with row and/or column covariates and colored cluster, R package version 2.2.0] from Bioconductor [41]. The Euclidean distance was used as distance function both for samples and genes. From the 299,563 genomic blocks, 7,384 blocks located in TSS200 CGIs were used for the clustering analysis because methylation of TSS200 CGIs is known to silence their downstream genes [12,38,39].

Statistical Analysis

Overall survival (OS) was calculated from the date of diagnosis to the date of death or the final date of survival confirmation. Survival curves were drawn by the Kaplan–Meier method, and were compared by the log-rank test. Fisher's exact test was used to evaluate a significant difference in an association between a pathway alteration and clinicopathological characteristics. All statistical analyses were conducted by PASW statistics version 18.0.0 (SPSS Japan, Inc., Tokyo, Japan).

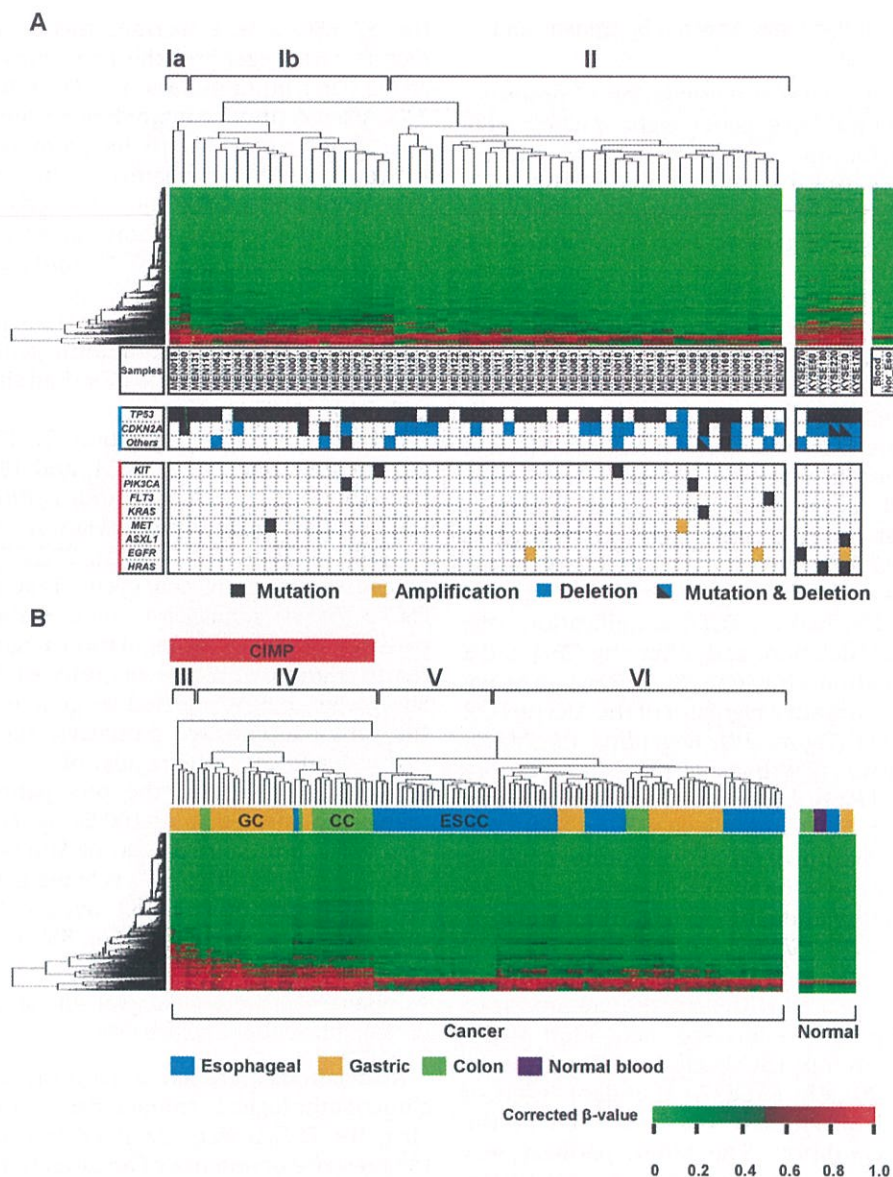


Figure 2. Associations between DNA methylation profile and gene mutations. (A) Unsupervised hierarchical clustering analysis using 7,384 genomic blocks with TSS200 CGIs. ESCCs in Clusters Ia and Ib had larger numbers of aberrantly methylated genes than those in Cluster II. Alterations of oncogenes and tumor suppressor genes were distributed in the three clusters with similar frequencies. (B)

Unsupervised hierarchical clustering analysis of 120 cancers (57 ESCCs, 43 gastric cancers, and 20 colon cancers). Cancers in Clusters III and IV had larger numbers of aberrantly methylated genes than those in Clusters V and VI. Cancers in Cluster VI had larger numbers of aberrantly methylated genes than those in Cluster V, rather resembling those in Cluster IV.

We further compared the numbers of aberrantly methylated genes with those in gastric and colon cancers, in which the presence of the CIMP is known [30,42–46]. Unsupervised hierarchical clustering analysis was conducted using corrected methylation profiles of 120 cancers, including the 57 ESCCs, 43 gastric cancers [47] (Supplementary Figure S3A), and 20 colon cancers (NCBI GEO DataSets; Accession no. GSE42752) [48] (Supplementary Figure S3B). The analysis produced four major clusters (Figure 2B). Interestingly, cancers of the same tissues formed

subclusters within the major clusters. In addition, gastric and colon cancers were split into Clusters IV and VI, which had a large and small, respectively, numbers of aberrantly methylated genes. ESCCs were in Clusters V and VI, both of which had a small number of aberrantly methylated genes, and cancers in clusters III and IV were considered CIMP positive. These results showed that the numbers of aberrantly methylated genes in ESCCs were smaller than those in gastric and colon cancers, and the CIMP is unlikely to be present in ESCCs.

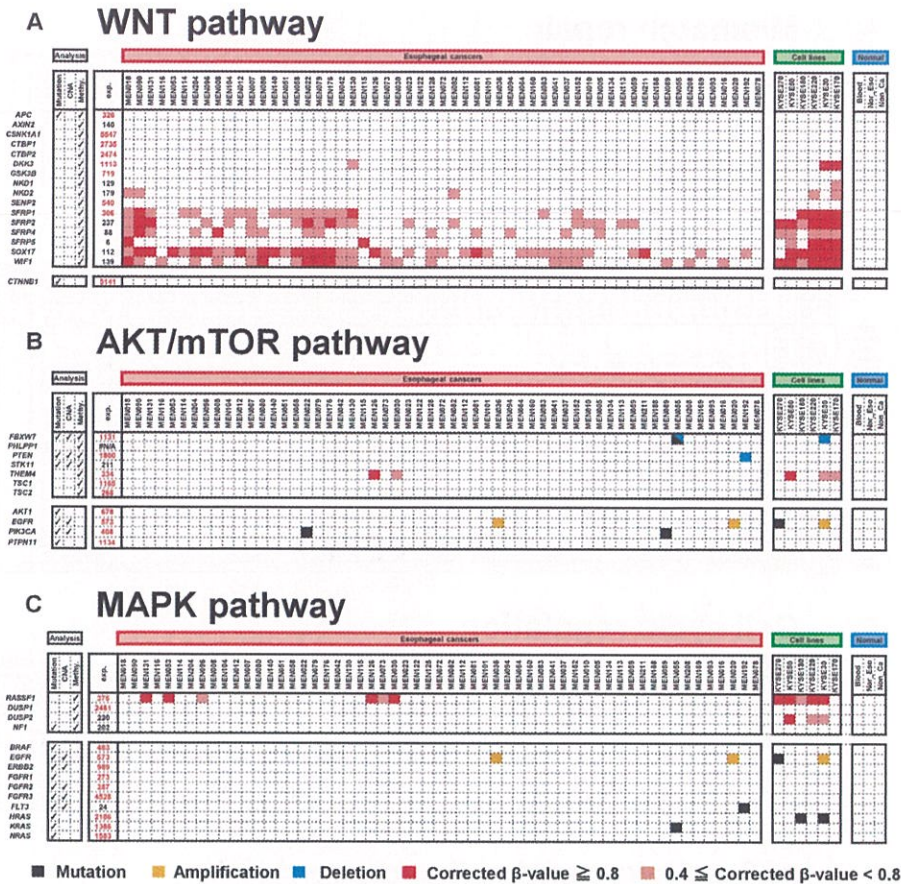


Figure 3. Genetic and epigenetic alterations in three growth-promoting pathways. (A) In the WNT pathway, none of the 57 ESCCs had an activating point mutation, but 19 ESCCs (33%) had heavy methylations of one or more of their 16 negative regulators. Expression levels obtained by microarray analysis of normal esophageal mucosae are also shown, and those higher than 250 are shown in red. Five of the six genes heavily methylated in ESCCs were not expressed in normal esophageal mucosae, suggesting that the five genes were methylated

as passenger genes. (B) In the AKT/mTOR pathway, two ESCCs (4%) had activating mutations of *PIK3CA*, two ESCCs (4%) had *EGFR* amplification, and one ESCC (2%) had a *PTEN* deletion. Only one ESCC (2%) had heavy methylation of *THEM4*. (C) In the MAPK pathway, two ESCCs (4%) had an amplification of *EGFR*, four (7%) had heavy methylation of *RASSF1*, and two (4%) had point mutations of *FLT3* and *KRAS*.

DISCUSSION

A genome-wide methylation analysis and an extensive mutation analysis of 57 ESCCs were conducted here, and they showed (i) that 44 of the 57 ESCCs (77%) had 64 non-synonymous somatic

mutations of 10 different potential driver genes (*ARID1A*, *CDKN2A*, *FBXW7*, *FLT3*, *KIT*, *KRAS*, *MET*, *MLH1*, *PIK3CA*, and *TP53*), (ii) that the number of aberrantly methylated genes in ESCCs was smaller than those in gastric and colon cancers, (iii) that ESCCs had at least one genetic or epigenetic alteration in the p53 pathway and cell cycle regulation with high frequencies (77% and 47%, respectively), and (iv) that 19 of the 57 ESCCs (33%) had heavy methylation of one gene or more of negative regulators in the WNT pathway. This is the first report in which genetic and epigenetic alterations were simultaneously analyzed in the same set of ESCC samples.

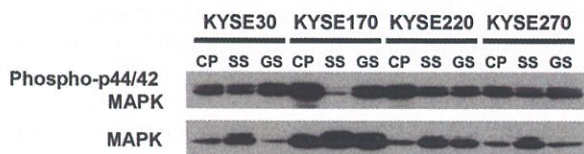


Figure 4. Activation of the MAPK pathway in ESCC cell lines. Phosphorylated MAPK and total MAPK levels were analyzed by Western blotting in four ESCC cell lines (KYSE30, KYSE170, KYSE220, and KYSE270) under conditions of cell proliferation (CP), serum-starvation (SS), and growth-stimulation (GS). In KYSE30, KYSE220, and KYSE270 abundant levels of phosphorylated MAPK were observed even in SS showing the MAPK pathway was constitutively activated. On the other hand, in KYSE170, only trace amounts of phosphorylated MAPK were observed in SS, showing the MAPK pathway was not activated.

Somatic mutations of six tumor-suppressor genes, four oncogenes, and CNVs of 10 genes were identified in this study. The most frequently mutated gene was *TP53* (70%), followed by *CDKN2A* (9%) and *PIK3CA* (4%) in this study, and the frequencies are close to the frequencies in the Catalogue of Somatic Mutations in

Table 1. Associations Between Pathways and Clinicopathological Findings

Category	Total number	Alterations in the WNT pathway			Alterations in the p53 pathway			Alterations in cell cycle regulation		
		Absent	Present	P-value*	Absent	Present	P-value*	Absent	Present	P-value*
Gender										
Male	51	33	18		11	40		25	26	
Female	6	5	1	0.652	2	4	0.610	3	3	1.000
Age										
<65	24	18	6		4	20		12	12	
≥65	33	20	13	0.394	9	24	0.524	16	17	1.000
Smoking										
Yes	51	33	18		10	41		24	27	
No	6	5	1	0.652	3	3	0.125	4	2	0.423
Drinking										
Yes	53	34	19		9	44		26	27	
No	4	4	0	0.290	4	0	0.002	2	2	1.000
Location										
Upper	9	7	6		2	7		7	2	
Middle	35	24	11		10	25		16	19	
Lower	13	7	2	0.468	1	12	0.309	5	8	0.156
T										
T1	12	6	6		3	9		5	7	
T2	8	6	2		1	7		6	2	
T3	36	25	11		9	27		16	20	
T4	1	1	0	0.498	0	1	0.823	1	0	0.288
N										
N0	10	6	4		2	8		6	4	
N1	47	32	15	0.717	11	36	1.000	22	25	0.504
M										
M0	43	31	12		9	34		24	19	
M1	14	7	7	0.192	4	10	0.715	4	10	0.123
Clinical stage										
IIA	8	5	3		2	6		5	3	
IIB	16	11	5		3	13		9	7	
III	19	15	4		4	15		10	9	
IVA/B	14	7	7	0.372	4	10	0.926	4	10	0.340

*P-values were calculated by Fisher's exact test. Bold value is statistic significant (smaller than 0.05).

genome-wide methylation profiles obtained here will provide a valuable source for future data mining for novel tumor-suppressor genes and diagnostic targets in ESCCs.

Among the tumor-suppressive pathways, the p53 pathway was most frequently affected (44/57; 77%). *TP53* was inactivated by genetic alterations (40/57; 70%), and its downstream gene, *MIR34B*, was inactivated by epigenetic alterations (6/57; 11%). Regarding cell cycle regulation, *CDKN2A* was methylated or mutated with a relatively low frequency (7/57; 6%), but deletions were frequently observed (17/50; 30%). A cell cycle checkpoint gene, *CHFR*, was methylated in a small fraction (4/57; 7%). In total, 27 ESCCs (47%) had deregulation of the cell cycle. Taken together, the majority of ESCCs (50/57; 88%) had at least one alteration of genes involved in the p53 pathway or cell cycle regulation (Figure 5D), showing that these pathways are deeply involved in ESCC development.

Regarding the mismatch repair, two ESCC had genetic alterations of *MLH1*, whereas none of the 57 ESCCs had aberrant methylation of *MLH1*, showing that mismatch repair is not frequently inactivated in ESCCs. This was in contrast with previous studies that reported the presence of aberrant methylation of *MLH1* in 6–62% of ESCCs by methylation-specific PCR [17,37,53]. The study here employed quantitative methylation analysis that excludes overestimation of aberrant methylation and analysis of a critical region for transcriptional silencing [12], and the discrepancy with previous studies may be attributed to these differences in the methods.

Among the three growth-promoting pathways, genetic alterations were not frequent. However, the WNT pathway was considered to be activated by methylation of its negative regulators (*SFRP1*, *SFRP2*, *SFRP4*, *SFRP5*, *SOX17*, and *WIF1*) in 19 ESCCs (33%). The finding was in line with previous studies that reported an association between aberrant

2. Rustgi AK, El-Serag HB. Esophageal carcinoma. *N Engl J Med* 2014;371:2499–2509.
3. Hu N, Wang C, Su H, et al. High frequency of CDKN2A alterations in esophageal squamous cell carcinoma from a high-risk Chinese population. *Genes Chromosomes Cancer* 2004;39:205–216.
4. Abedi-Ardekani B, Dar NA, Mir MM, et al. Epidermal growth factor receptor (EGFR) mutations and expression in squamous cell carcinoma of the esophagus in central Asia. *BMC Cancer* 2012;12:602.
5. Kim YR, Oh JE, Kim MS, et al. Oncogenic NRF2 mutations in squamous cell carcinomas of oesophagus and skin. *J Pathol* 2010;220:446–451.
6. Mori R, Ishiguro H, Kimura M, et al. PIK3CA mutation status in Japanese esophageal squamous cell carcinoma. *J Surg Res* 2008;145:320–326.
7. Maeng CH, Lee J, van Hummelen P, et al. High-throughput genotyping in metastatic esophageal squamous cell carcinoma identifies phosphoinositide-3-kinase and BRAF mutations. *PLoS ONE* 2012;7:e41655.
8. Agrawal N, Jiao Y, Bettgeowda C, et al. Comparative genomic analysis of esophageal adenocarcinoma and squamous cell carcinoma. *Cancer Discov* 2012;2:899–905.
9. Song Y, Li L, Ou Y, et al. Identification of genomic alterations in oesophageal squamous cell cancer. *Nature* 2014;509:91–95.
10. Lin DC, Hao JJ, Nagata Y, et al. Genomic and molecular characterization of esophageal squamous cell carcinoma. *Nature Genet* 2014;46:467–473.
11. Gao YB, Chen ZL, Li JG, et al. Genetic landscape of esophageal squamous cell carcinoma. *Nat Genet* 2014;46:1097–1102.
12. Ushijima T. Detection and interpretation of altered methylation patterns in cancer cells. *Nat Rev Cancer* 2005;5:223–231.
13. Kalari S, Pfeifer GP. Identification of driver and passenger DNA methylation in cancer by epigenomic analysis. *Adv Genet* 2010;70:277–308.
14. Nephew KP, Huang TH. Epigenetic gene silencing in cancer initiation and progression. *Cancer Lett* 2003;190:125–133.
15. Lee YC, Wang HP, Wang CP, et al. Revisit of field cancerization in squamous cell carcinoma of upper aerodigestive tract: Better risk assessment with epigenetic markers. *Cancer Prev Res (Phila)* 2011;4:1982–1992.
16. Esteller M. CpG island hypermethylation and tumor suppressor genes: A booming present, a brighter future. *Oncogene* 2002;21:5427–5440.
17. Guo M, Ren J, House MG, Qi Y, Brock MV, Herman JG. Accumulation of promoter methylation suggests epigenetic progression in squamous cell carcinoma of the esophagus. *Clin Cancer Res* 2006;12:4515–4522.
18. Lee EJ, Lee BB, Han J, et al. CpG island hypermethylation of E-cadherin (CDH1) and integrin alpha4 is associated with recurrence of early stage esophageal squamous cell carcinoma. *Int J Cancer* 2008;123:2073–2079.
19. Fukuoka T, Hibi K, Nakao A. Aberrant methylation is frequently observed in advanced esophageal squamous cell carcinoma. *Anticancer Res* 2006;26:3333–3335.
20. Li B, Wang B, Niu LJ, Jiang L, Qiu CC. Hypermethylation of multiple tumor-related genes associated with DNMT3b up-regulation served as a biomarker for early diagnosis of esophageal squamous cell carcinoma. *Epigenetics* 2011;6:307–316.
21. Kim YT, Park JY, Jeon YK, et al. Aberrant promoter CpG island hypermethylation of the adenomatous polyposis coli gene can serve as a good prognostic factor by affecting lymph node metastasis in squamous cell carcinoma of the esophagus. *Dis Esophagus* 2009;22:143–150.
22. Kuroki T, Trapasso F, Yendamuri S, et al. Promoter hypermethylation of RASSF1A in esophageal squamous cell carcinoma. *Clin Cancer Res* 2003;9:1441–1445.
23. Mao WM, Li P, Zheng QQ, et al. Hypermethylation-modulated downregulation of RASSF1A expression is associated with the progression of esophageal cancer. *Arch Med Res* 2011;42:182–188.
24. Takeno S, Noguchi T, Fumoto S, Kimura Y, Shibata T, Kawahara K. E-cadherin expression in patients with esophageal squamous cell carcinoma: Promoter hypermethylation, Snail overexpression, and clinicopathologic implications. *Am J Clin Pathol* 2004;122:78–84.
25. Xing EP, Nie Y, Wang LD, Yang GY, Yang CS. Aberrant methylation of p16INK4a and deletion of p15INK4b are frequent events in human esophageal cancer in Linxian, China. *Carcinogenesis* 1999;20:77–84.
26. Zare M, Jazii FR, Alivand MR, Nasserri NK, Malekzadeh R, Yazdanbod M. Qualitative analysis of Adenomatous Polyposis Coli promoter: Hypermethylation, engagement and effects on survival of patients with esophageal cancer in a high risk region of the world, a potential molecular marker. *BMC Cancer* 2009;9:24.
27. Sobin LH. TNM classification of malignant tumors. 6th edition. In: Sobin LH, editor. New York: Wiley-Blackwell; 2002.
28. Takahashi T, Matsuda Y, Yamashita S, et al. Estimation of the fraction of cancer cells in a tumor DNA sample using DNA methylation. *PLoS ONE* 2013;8:e82302.
29. Shimada Y, Imamura M, Wagata T, Yamaguchi N, Tobe T. Characterization of 21 newly established esophageal cancer cell lines. *Cancer* 1992;69:277–284.
30. Kim JG, Takeshima H, Niwa T, et al. Comprehensive DNA methylation and extensive mutation analyses reveal an association between the CpG island methylator phenotype and oncogenic mutations in gastric cancers. *Cancer Lett* 2013;330:33–40.
31. Yamada M, Fukagawa T, Nakajima T, et al. Hereditary diffuse gastric cancer in a Japanese family with a large deletion involving CDH1. *Gastric Cancer* 2014;17:750–756.
32. Takeshima H, Yamashita S, Shimazu T, Niwa T, Ushijima T. The presence of RNA polymerase II, active or stalled, predicts epigenetic fate of promoter CpG islands. *Genome Res* 2009;19:1974–1982.
33. Shigematsu Y, Niwa T, Yamashita S, et al. Identification of a DNA methylation marker that detects the presence of lymph node metastases of gastric cancers. *Oncol Lett* 2012;4:268–274.
34. Lea IA, Jackson MA, Li X, Bailey S, Peddada SD, Dunnick JK. Genetic pathways and mutation profiles of human cancers: Site- and exposure-specific patterns. *Carcinogenesis* 2007;28:1851–1858.
35. Hildebrandt MA, Yang H, Hung MC, et al. Genetic variations in the PI3K/PTEN/AKT/mTOR pathway are associated with clinical outcomes in esophageal cancer patients treated with chemoradiotherapy. *J Clin Oncol* 2009;27:857–871.
36. Jia Y, Yang Y, Zhan Q, et al. Inhibition of SOX17 by microRNA 141 and methylation activates the WNT signaling pathway in esophageal cancer. *J Mol Diagn* 2012;14:577–585.
37. Tzao C, Hsu HS, Sun GH, et al. Promoter methylation of the hMLH1 gene and protein expression of human mutL homolog 1 and human mutS homolog 2 in resected esophageal squamous cell carcinoma. *J Thorac Cardiovasc Surg* 2005;130:1371.
38. Jones PA, Baylin SB. The epigenomics of cancer. *Cell* 2007;128:683–692.
39. Lin JC, Jeong S, Liang G, et al. Role of nucleosomal occupancy in the epigenetic silencing of the MLH1 CpG island. *Cancer cell* 2007;12:432–444.
40. Miyakura Y, Sugano K, Konishi F, et al. Extensive methylation of hMLH1 promoter region predominates in proximal colon cancer with microsatellite instability. *Gastroenterology* 2001;121:1300–1309.
41. Gentleman RC, Carey VJ, Bates DM, et al. Bioconductor: open software development for computational biology and bioinformatics. *Genome Biol* 2004;5:R80.

1 Supplemental Files

2

3 *Supplemental file 1: Table S1: Clinical features of the 57 ESCC cases.*4 *Supplemental file 2: Table S2: List of 55 cancer-related genes.*5 *Supplemental file 3: Table S3: Primers used for dideoxy sequencing.*6 *Supplemental file 4: Table S4: List of 81 genes of cancer-related pathways.*7 *Supplemental file 5: Table S5: List of the positions of CpG sites.*8 *Supplemental file 6: Table S6: Variations identified in the 57 ESCCs.*9 *Supplemental file 7: Table S7: Relative reading depth of the 28 genes to the reference in the*
10 *57 ESCCs.*

11

12 *Supplemental file 8: Figure S1 The number of genes for the three kinds of analyses.*13 A total of 81 genes were selected for analyses of the six cancer-related pathways. Among
14 the 81 genes, 25 genes were analyzed for base substitutions, 67 genes for methylation-
15 silencing, and 11 genes for both. Among the 25 genes, 14 genes were analyzed for CNAs,
16 and eight genes were analyzed for base substitutions, CNAs, and methylation-silencing.

17

18 *Supplemental file 9: Figure S2 Detection of CNA by Ion PGM sequencer.*19 (A) Representative scattered plots of reading depth of the target regions between the ESCC
20 and noncancerous mucosae. The slope shows RRDR. Red squares denote the eight target
21 regions on *EGFR*. (B) Array-CGH data around the *EGFR* regions. Y-axis with boxes shows
22 genomic locations. X-axis shows relative signal intensity (rSI) of the probes to the reference
23 DNA. A number in the chart indicates an average of signal intensity of the probes in the
24 target gene. (C) RRDR and rSI of *EGFR* and *CDKN2A* in three ESCCs (Round plots; RRDR,
25 Square plots; rSI).

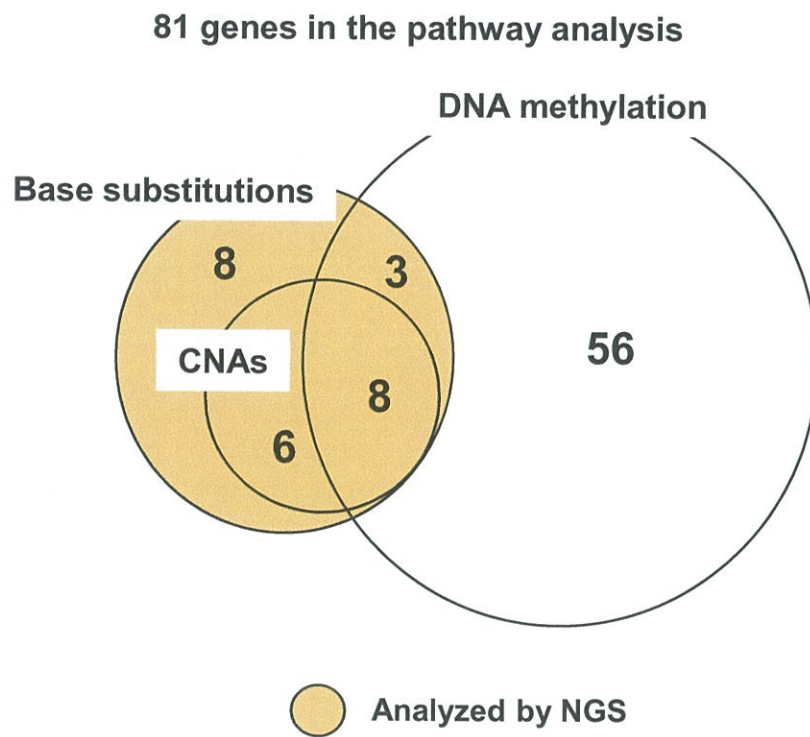


Figure S1
Kishino *et al.*

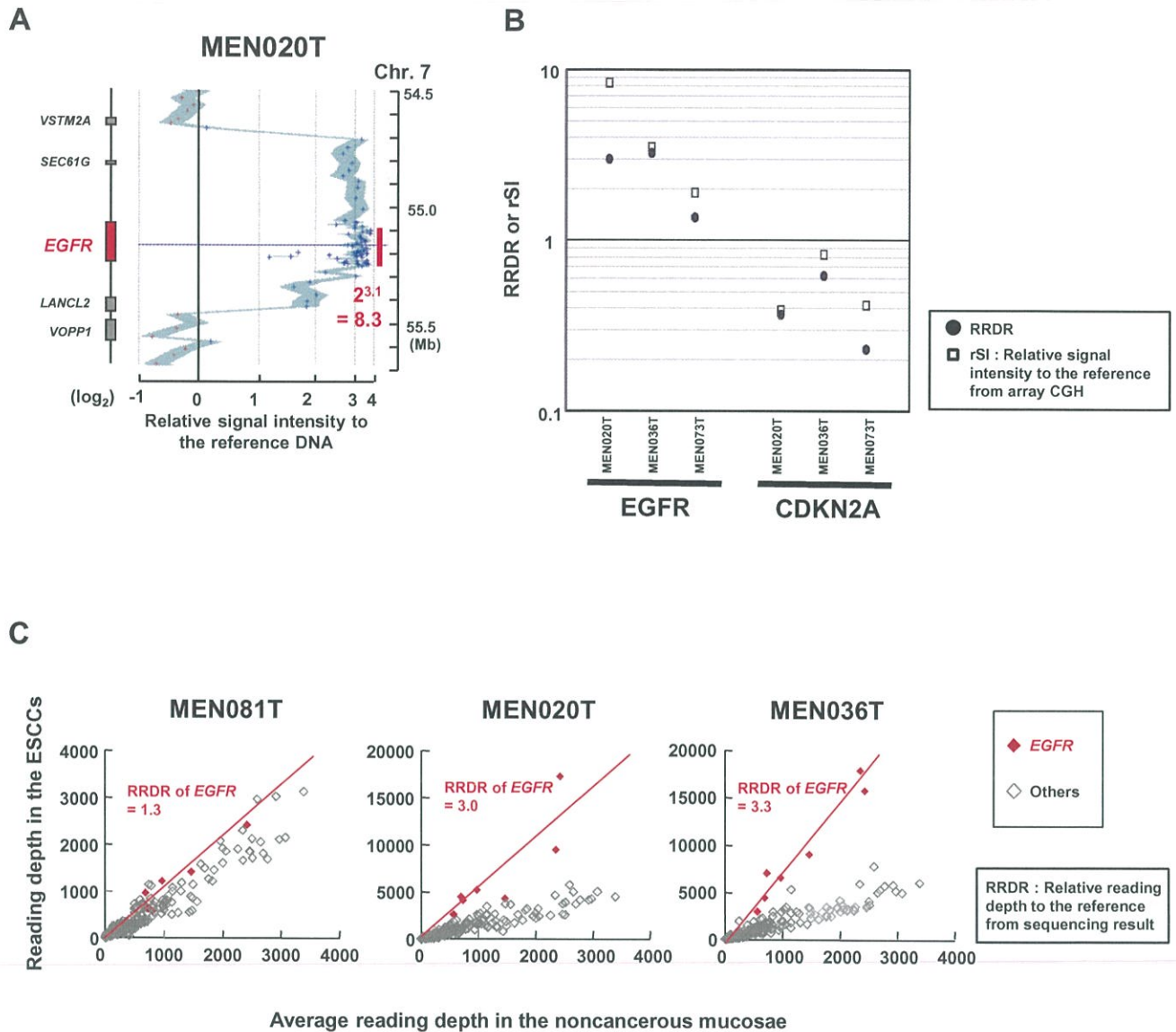


Figure S2
Kishino et al.

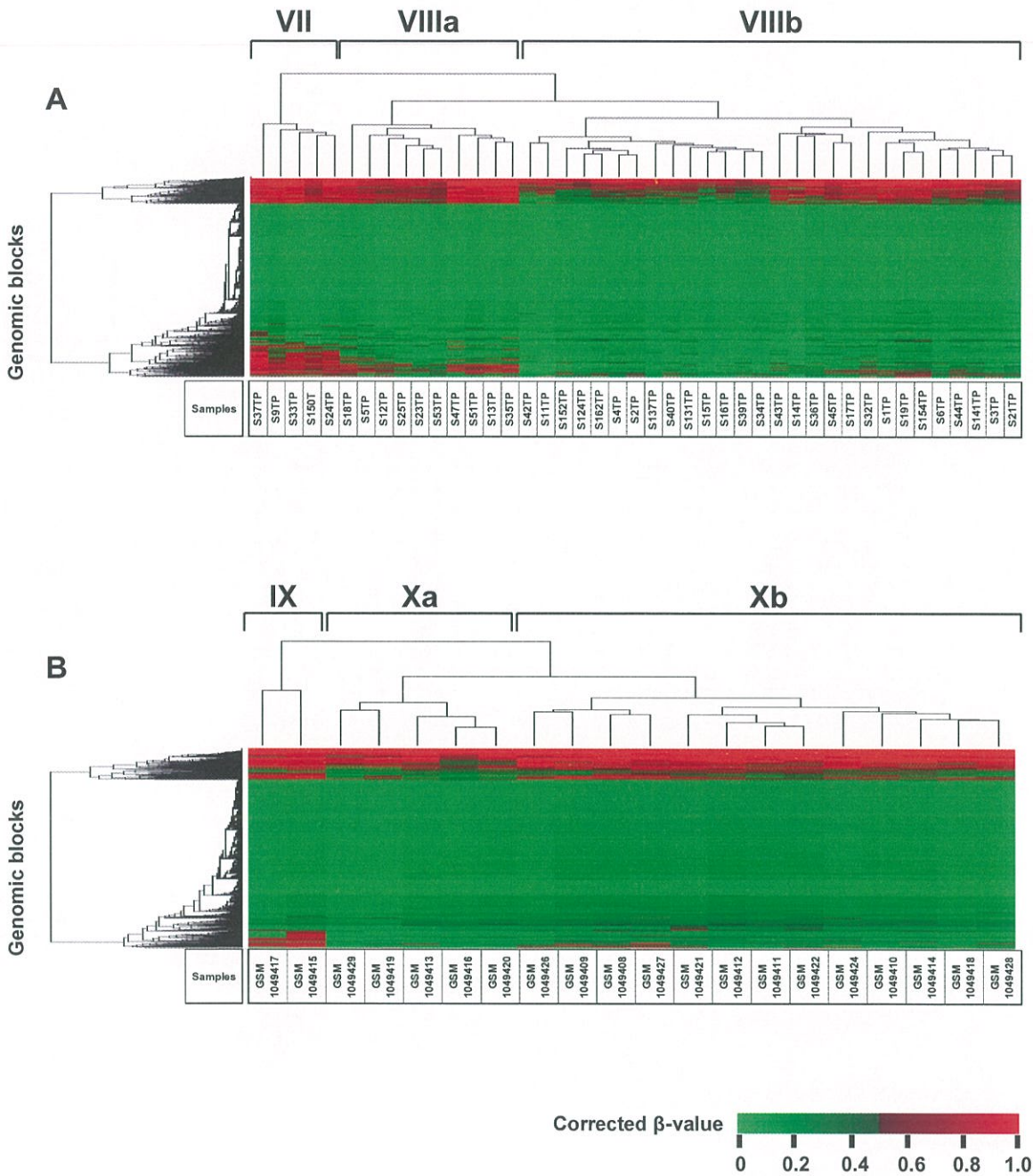


Figure S3
Kishino *et al.*

Table S1. Clinical features of the 57 ESCC cases

Sample	Individual				Tumor (clinical diagnosis) UICC 6th				
	Age	Gender	Smoking	Drinking	Location	T	N	M	cStage
MEN005	66	M	Yes	Yes	Mt	T3	N1	M0	III
MEN007	68	M	Yes	Yes	Lt	T1b	N1	M0	IIB
MEN008	61	M	Yes	Yes	Lt	T3	N1	M0	III
MEN010	74	M	Yes	Yes	Lt	T1b	N1	M0	IIB
MEN012	68	M	Yes	Yes	Lt	T1b	N0	M1b	IVB
MEN016	63	F	Yes	Yes	Mt	T3	N1	M0	III
MEN018	63	M	Yes	Yes	Mt	T3	N1	M1b	IVB
MEN020	56	M	Yes	Yes	Mt	T3	N1	M1b	IVB
MEN022	68	M	Yes	Yes	Mt	T1b	N1	M0	IIB
MEN023	61	M	Yes	Yes	Lt	T3	N1	M0	III
MEN030	49	M	Yes	Yes	Mt	T2	N1	M0	IIB
MEN036	63	M	Yes	Yes	Mt	T3	N1	M0	III
MEN037	64	M	Yes	Yes	Mt	T2	N0	M0	IIA
MEN041	65	M	Yes	Yes	Mt	T3	N1	M0	III
MEN042	70	M	Yes	Yes	Mt	T3	N1	M0	III
MEN051	75	M	Yes	No	Mt	T3	N1	M1b	IVB
MEN053	77	M	Yes	Yes	Mt	T2	N0	M0	IIA
MEN055	64	M	Yes	Yes	Ce	T3	N0	M1b	IVB
MEN058	58	M	Yes	Yes	Mt	T3	N0	M0	IIA
MEN059	67	M	Yes	Yes	Lt	T3	N0	M0	IIA
MEN064	66	M	Yes	Yes	Ce	T2	N1	M0	IIB
MEN072	61	F	Yes	Yes	Lt	T1b	N1	M0	IIB
MEN073	70	F	No	No	Mt	T3	N1	M0	III
MEN078	48	M	No	Yes	Mt	T1b	N1	M0	IIB
MEN079	69	M	Yes	Yes	Mt	T3	N0	M0	IIA
MEN080	67	M	Yes	Yes	Lt	T3	N1	M0	III
MEN081	66	M	Yes	Yes	Mt	T1b	N1	M1b	IVB
MEN082	67	M	Yes	Yes	Mt	T3	N1	M0	III
MEN083	75	M	Yes	Yes	Mt	T1b	N1	M0	IIB
MEN089	62	F	Yes	Yes	Mt	T3	N1	M0	III
MEN090	70	M	Yes	Yes	Mt	T3	N1	M1b	IVB
MEN093	58	M	Yes	Yes	Mt	T3	N1	M0	III
MEN094	60	M	Yes	Yes	Mt	T3	N0	M0	IIA
MEN096	73	M	Yes	Yes	Lt	T3	N1	M0	III
MEN101	65	M	Yes	Yes	Mt	T3	N1	M1b	IVB
MEN104	57	M	Yes	Yes	Ut	T4	N1	M0	III
MEN112	68	F	No	Yes	Mt	T3	N1	M0	III
MEN113	69	M	Yes	Yes	Ut	T3	N0	M0	IIA
MEN114	70	M	Yes	Yes	Lt	T3	N1	M0	III
MEN115	67	F	Yes	Yes	Mt	T1b	N1	M0	IIB
MEN116	64	M	Yes	Yes	Mt	T2	N1	M0	IIB
MEN122	69	M	No	No	Ut	T3	N0	M0	IIA
MEN126	69	M	Yes	Yes	Mt	T3	N1	M1b	IVB
MEN128	70	M	Yes	Yes	Ut	T2	N1	M0	IIB
MEN130	74	M	Yes	Yes	Ut	T1b	N1	M0	IIB
MEN131	60	M	No	Yes	Ut	T2	N1	M0	IIB
MEN134	79	M	Yes	Yes	Lt	T3	N1	M0	III
MEN140	75	M	Yes	Yes	Ae	T3	N1	M1a	IVA
MEN152	55	M	Yes	Yes	Mt	T3	N1	M1b	IVB
MEN160	64	M	Yes	Yes	Mt	T2	N1	M0	IIB
MEN169	79	M	Yes	Yes	Ut	T3	N1	M0	III
MEN176	54	M	Yes	Yes	Lt	T3	N1	M1b	IVB
MEN188	56	M	Yes	Yes	Mt	T3	N1	M1b	IVB
MEN192	67	M	No	No	Mt	T1b	N1	M0	IIB
MEN204	65	M	Yes	Yes	Mt	T1b	N1	M0	IIB
MEN208	61	M	Yes	Yes	Mt	T3	N1	M1b	IVB
MEN211	55	M	Yes	Yes	Mt	T3	N1	M0	III

Table S2. List of 55 cancer-related genes.

Gene	Base substitution	CNA	Pathway
<i>ABL1</i>	✓	✓	
<i>AKT1</i>	✓		✓
<i>ALK</i>	✓		
<i>APC</i>	✓	✓	✓
<i>ARID1A</i>	✓		
<i>ASXL1</i>	✓	✓	
<i>ATM</i>	✓	✓	
<i>BRAF</i>	✓		✓
<i>BRCA1</i>	✓		
<i>CDH1</i>	✓	✓	
<i>CDKN2A</i>	✓	✓	✓
<i>CSF1R</i>	✓		
<i>CTNNB1</i>	✓		✓
<i>EGFR</i>	✓	✓	✓
<i>EP300</i>	✓		
<i>ERBB2</i>	✓	✓	✓
<i>ERBB4</i>	✓	✓	
<i>FBXW7</i>	✓	✓	✓
<i>FGFR1</i>	✓		✓
<i>FGFR2</i>	✓	✓	✓
<i>FGFR3</i>	✓	✓	✓
<i>FLT3</i>	✓	✓	✓
<i>GNAS</i>	✓		
<i>H3F3A</i>	✓		
<i>HNF1A</i>	✓		
<i>HRAS</i>	✓		✓
<i>IDH1</i>	✓		
<i>JAK2</i>	✓		
<i>JAK3</i>	✓		
<i>KDR</i>	✓	✓	
<i>KIT</i>	✓	✓	
<i>KRAS</i>	✓		✓
<i>MET</i>	✓	✓	
<i>MLH1</i>	✓	✓	✓
<i>MLL3</i>	✓	✓	
<i>MPL</i>	✓		
<i>MSH2</i>	✓		✓
<i>MSH6</i>	✓		✓
<i>NF1</i>	✓		✓
<i>NOTCH1</i>	✓		
<i>NPM1</i>	✓		
<i>NRAS</i>	✓		✓
<i>PDGFRA</i>	✓	✓	
<i>PIK3CA</i>	✓	✓	✓
<i>PTEN</i>	✓	✓	✓
<i>PTPN11</i>	✓		✓
<i>RB1</i>	✓	✓	✓
<i>RET</i>	✓	✓	
<i>SMAD4</i>	✓	✓	

Table S5. List of the positions of CpG sites.

ID of a block	Gene	Relation to a TSS	Island	Signaling pathway	# of CpG sites	Chromosome	Positions of probes
78446	FEAX7	TSS200	Island	Akt/mTOR	4	4	153456344, 153456325, 153456176, 153456369
258340	PHLP1	TSS200	Island	Akt/mTOR	6	18	60382541, 60382543, 60382673, 60382585, 60382658, 60382639
160869	PTEN	TSS200	Island	Akt/mTOR	10	10	80623020, 80623157, 80623018, 80623122, 80623013, 80623071, 80623004, 80623076, 80623138, 80623142
18501	THM4	TSS200	Island	Akt/mTOR	4	1	151882284, 151882157, 151882143, 151882287
260052	STK11	TSS200	Island	Akt/mTOR	3	19	1205696, 1205706, 1205715
151071	STK1	5'UTR	Island	Akt/mTOR	1	9	153819856
227733	TSC2	TSS200	Island	Akt/mTOR	1	16	2097837
145721	CDKN2A (p16)	Intron	Island	Cell cycle	9	9	21924704
199530	CIFR	TSS200	Island	Cell cycle	4	12	132464357, 132464323, 132464351, 132464327
103652	CDKN1A	Island	Island	Cell cycle	1	5	3664390
168878	CDKN1C	TSS200	Island	Cell cycle	1	11	2907008
145727	CDKN2B	TSS200	Island	Cell cycle	1	9	2209355
186669	CDKN1B	TSS200	Island	Cell cycle	2	12	12870119, 12870121
116646	CDKN1C	TSS200	Island	Cell cycle	5	1	51434293, 51434354, 51434335
263673	CDKN2D	TSS200	Island	Cell cycle	1	1	16302665
4967	ZBTB17	TSS200	Island	Cell cycle	1	1	16302665
56277	RASSF1	TSS200	Island	MAPK	7	3	50378529, 50378413, 50378407, 50378425, 50378527, 50378423, 50378431
94194	DUSP1	TSS200	Island	MAPK	1	5	172198326
38242	DUSP2	TSS200	Island	MAPK	1	2	96811264
244901	NF1	TSS200	Island	MAPK	7	17	29421884, 29421871, 29421804, 29421766, 29421766, 29421851, 29421890, 29421832
54358	MLH1	TSS200	Island	Mismatch repair	2	3	370344814, 37034825
54363	MH1	TSS200	Island	Mismatch repair	8	3	3703205, 3703228, 3703222, 3703200, 37035168, 37035158, 37035220, 37035207
34098	MSH2	TSS200	Island	Mismatch repair	4	2	47630251, 47630224, 47630147, 47630172
86775	MSH3	TSS200	Island	Mismatch repair	1	5	79950120
34551	MSH6	TSS200	Island	Mismatch repair	3	2	48010097, 48010117, 48010105
45463	PHM3	TSS200	Island	Mismatch repair	3	2	19048631, 19048634, 19048693
116765	PHM3	TSS200	Island	Mismatch repair	3	7	6048868, 6048832, 6048875
271621	BAX	TSS200	Island	p53	2	19	49458001, 49457927
80178	CASP3	TSS200	Island	p53	1	4	135570637
172789	COR2	TSS200	Island	p53	6	11	44586959, 44587138, 44587057, 44586968, 44587077, 44587044
103652	CDKN1A	TSS200	Island	p53	1	6	36646390
283595	CHEK2	TSS200	Island	p53	6	22	29137963, 29137974, 29137974, 29137992, 29137984, 29137908
118141	CYC5	TSS200	Island	p53	4	7	25164991, 25164974, 25165070, 25164994
172357	DDP2	TSS200	Island	p53	2	11	47236414, 47236405
183239	EBF4	TSS200	Island	p53	4	11	125439225, 125439223, 125439275, 125439230
260892	GADD45B	TSS200	Island	p53	3	19	2476132, 2476129, 2476077
147500	GADD45G	TSS200	Island	p53	1	9	92219858
288368	GISE1	TSS200	Island	p53	5	22	46692606, 46692562, 46692594, 46692631, 46692564
73534	IGFBP7	TSS200	Island	p53	4	4	57976561, 57976573, 57976566, 57976556
110666	MIR34B	TSS200	Island	p53	5	11	111383603, 111383576, 111383515, 111383624, 111383653
110508	PRP2	TSS200	Island	p53	4	6	138428740, 138428736, 138428792, 138428533
258255	PAH1P1	TSS200	Island	p53	5	18	57651000, 57651199, 57651154, 57651158, 57651007
42917	ROR1	TSS200	Island	p53	5	2	15435396, 15435358, 15435379, 15435384, 15435348
30744	RBM2	TSS200	Island	p53	6	2	10262814, 10262820, 10262827, 10262822, 10262861, 10262787
108481	SESN1	TSS200	Island	p53	4	6	109416237, 109416235, 109416242, 109416245
7869	SESN2	TSS200	Island	p53	1	28383832, 28383863, 28383837, 28383917	
232849	SHH1	TSS200	Island	p53	2	16	48399813, 48399834
40448	STEAP3	TSS200	Island	p53	4	2	119981334, 119981253, 119981284, 119981187
218061	THBS1	TSS200	Island	p53	4	15	39873206, 39873260, 39873258, 39873209
134964	TNFRSF10B	TSS200	Island	p53	5	8	22926785, 22926698, 22926860, 22926862, 22926800
65741	ZMAT3	TSS200	Island	p53	3	3	178789707, 178789612, 178789599
88286	APC	TSS200	Island	WNT	8	5	112043137, 112043105, 112043080, 112043158, 112043117, 112043188, 112043194
251203	AXIN2	TSS200	Island	WNT	1	17	63557887
92724	CNN3	TSS200	Island	WNT	6	6	448931078, 448931071, 448931119, 448931087, 448931203, 448931083
68746	CITR1	TSS200	Island	WNT	1	4	243087
165340	CITR2	TSS200	Island	WNT	5	10	126849762, 126849780, 126849704, 126849760, 126849624
170342	DKF3	TSS200	Island	WNT	6	11	12030268, 12030276, 12030375, 12030187, 12030272, 12030289
60841	GSK3B	TSS200	Island	WNT	3	3	19813301, 19813316, 19813310
23102	GSK3A	TSS200	Island	WNT	2	16	50582193, 50582056
81362	NKD1	TSS200	Island	WNT	1	5	1090991
66546	SENP2	TSS200	Island	WNT	4	3	183303994, 183303998, 183303988, 183303959
136777	SFRP1	TSS200	Island	WNT	5	8	41167087, 41167113, 41167109, 41167107, 41166990
78637	SFRP2	TSS200	Island	WNT	7	4	154710353, 154710418, 154710371, 154710399, 154710421, 154710425, 154710373
119632	SFRP4	TSS200	Island	WNT	1	7	37956554
162008	SFRP5	TSS200	Island	WNT	6	10	99531765, 99531879, 99531934, 99531790, 99531929, 99531929
137633	SOX17	TSS200	Island	WNT	6	8	55370423, 55370429, 55370434, 55370334, 55370407, 55370336
191965	WIF1	TSS200	Island	WNT	2	12	65515290, 65515276

Among the genes involved in the AKT/mTOR, MAPK, WNT pathways, mismatch repair, cell cycle regulation, and the p53 pathway, genes with genomic blocks within TSS200 CGIs were selected from the Kyoto Encyclopedia of Genes and Genomes (KEGG) Pathway Database.

Table S6. Variations identified in the 57 ESCCs.

Sample name	Gene	Chromosome	Region	Coverage	Frequency(%)	Coding region change	Amino acid change	Type	Zygosity
MEN007	<i>TP53</i>	chr17	7577120	2988	31.8	c.818G>T	p.Arg273Leu	SNV	Heterozygous
MEN008	<i>TP53</i>	chr17	7578271	360	30.3	c.578A>C	p.His193Pro	SNV	Heterozygous
MEN010	<i>TP53</i>	chr17	7577538	614	37.6	c.743G>A	p.Arg248Gln	SNV	Heterozygous
MEN010	<i>KIT</i>	chr4	55593461	191	42.4	c.1618G>C	p.Val540Leu	SNV	Heterozygous
MEN012	<i>TP53</i>	chr17	7578263	862	18.9	c.586C>T	p.Arg196*	SNV	Heterozygous
MEN018	<i>TP53</i>	chr17	7577573	1036	66.3	c.708C>A	p.Tyr236*	SNV	Heterozygous
MEN020	<i>TP53</i>	chr17	7577098	1883	27.1	c.840A>T	p.Arg280Ser	SNV	Heterozygous
MEN022	<i>TP53</i>	chr17	7578438^7578439	474	69.4	c.491_492insAA	p.Lys164fs	Insertion	Heterozygous
MEN022	<i>MLH1</i>	chr3	37067242	687	78.0	c.1153C>T	p.Arg385Cys	SNV	Heterozygous
MEN022	<i>PIK3CA</i>	chr3	178936082	923	35.4	c.1624G>A	p.Glu542Lys	SNV	Heterozygous
MEN023	<i>TP53</i>	chr17	7578190	695	56.4	c.659A>G	p.Tyr220Cys	SNV	Heterozygous
MEN030	<i>TP53</i>	chr17	7579358	79	64.6	c.329G>T	p.Arg110Leu	SNV	Heterozygous
MEN036	<i>TP53</i>	chr17	7577121	2169	30.3	c.817C>T	p.Arg273Cys	SNV	Heterozygous
MEN037	<i>TP53</i>	chr17	7577046	2556	69.5	c.892G>T	p.Glu298*	SNV	Heterozygous
MEN041	<i>TP53</i>	chr17	7577127	2308	34.4	c.811G>A	p.Glu271Lys	SNV	Heterozygous
MEN041	<i>TP53</i>	chr17	7578412	624	31.7	c.518T>A	p.Val173Glu	SNV	Heterozygous
MEN042	<i>TP53</i>	chr17	7577121	2202	13.6	c.817C>T	p.Arg273Cys	SNV	Heterozygous
MEN042	<i>TP53</i>	chr17	7577124	1907	18.2	c.814G>A	p.Val272Met	SNV	Heterozygous
MEN042	<i>KIT</i>	chr4	55593461	175	41.1	c.1618G>C	p.Val540Leu	SNV	Heterozygous
MEN051	<i>CDKN2A</i>	chr9	21971159	170	37.6	c.242G>C	p.Arg81Pro	SNV	Heterozygous
MEN053	<i>TP53</i>	chr17	7579358	118	39.0	c.329G>T	p.Arg110Leu	SNV	Heterozygous
MEN055	<i>KRAS</i>	chr12	25378562	3482	28.4	c.436G>A	p.Ala146Thr	SNV	Heterozygous
MEN055	<i>TP53</i>	chr17	7577546..7577547	378	63.2	c.734_735delGC	p.Gly245fs	Deletion	Heterozygous
MEN055	<i>FBXW7</i>	chr4	153259008	64	65.6	c.807delG	p.Met269fs	Deletion	Heterozygous
MEN055	<i>CDKN2A</i>	chr9	21971170^21971171	616	67.0	c.230_231insCCTGC	p.Ala77fs	Insertion	Heterozygous
MEN059	<i>TP53</i>	chr17	7578443	262	47.3	c.487T>A	p.Tyr163Asn	SNV	Heterozygous
MEN072	<i>TP53</i>	chr17	7578190	372	79.0	c.659A>G	p.Tyr220Cys	SNV	Heterozygous
MEN079	<i>TP53</i>	chr17	7577579	297	47.5	c.702C>A	p.Tyr234*	SNV	Heterozygous
MEN080	<i>TP53</i>	chr17	7577124	395	23.0	c.814G>A	p.Val272Met	SNV	Heterozygous
MEN080	<i>TP53</i>	chr17	7578264^7578265	210	30.0	c.584_585insT	p.Ile195fs	Insertion	Heterozygous
MEN080	<i>CDKN2A</i>	chr9	21971186	98	52.0	c.215C>T	p.Pro72Leu	SNV	Heterozygous
MEN082	<i>TP53</i>	chr17	7578445	305	25.2	c.485T>G	p.Ile162Ser	SNV	Heterozygous
MEN089	<i>PIK3CA</i>	chr3	178936082	685	22.5	c.1624G>A	p.Glu542Lys	SNV	Heterozygous
MEN090	<i>TP53</i>	chr17	7577538	534	19.9	c.743G>A	p.Arg248Gln	SNV	Heterozygous
MEN090	<i>CDKN2A</i>	chr9	21974742	201	35.8	c.85C>G	p.Arg29Gly	SNV	Heterozygous
MEN090	<i>CDKN2A</i>	chr9	21974744	201	35.8	c.83T>C	p.Val28Ala	SNV	Heterozygous
MEN093	<i>TP53</i>	chr17	7574003	940	41.8	c.1024C>T	p.Arg342*	SNV	Heterozygous
MEN094	<i>TP53</i>	chr17	7578271	547	17.0	c.578A>T	p.His193Leu	SNV	Heterozygous
MEN096	<i>TP53</i>	chr17	7577547	661	31.8	c.734G>A	p.Gly245Asp	SNV	Heterozygous
MEN101	<i>TP53</i>	chr17	7578190	212	38.7	c.659A>G	p.Tyr220Cys	SNV	Heterozygous
MEN104	<i>TP53</i>	chr17	7578235	521	22.5	c.614A>G	p.Tyr205Cys	SNV	Heterozygous
MEN104	<i>MET</i>	chr7	116339673	682	15.8	c.535G>A	p.Ala179Thr	SNV	Heterozygous
MEN112	<i>TP53</i>	chr17	7577094	2227	28.5	c.844C>T	p.Arg282Trp	SNV	Heterozygous
MEN112	<i>TP53</i>	chr17	7578239	475	32.8	c.610G>T	p.Glu204*	SNV	Heterozygous
MEN113	<i>TP53</i>	chr17	7577130	1109	50.8	c.808T>A	p.Phe270Ile	SNV	Heterozygous
MEN113	<i>TP53</i>	chr17	7577577	637	34.7	c.704delA	p.Asn235fs	Deletion	Heterozygous
MEN115	<i>TP53</i>	chr17	7578190	541	67.5	c.659A>G	p.Tyr220Cys	SNV	Heterozygous
MEN116	<i>TP53</i>	chr17	7577558	689	50.2	c.723delC	p.Ser241fs	Deletion	Heterozygous
MEN126	<i>TP53</i>	chr17	7578479	297	87.9	c.451C>T	p.Pro151Ser	SNV	Heterozygous
MEN128	<i>TP53</i>	chr17	7577538	1052	54.6	c.743G>A	p.Arg248Gln	SNV	Heterozygous
MEN130	<i>TP53</i>	chr17	7578406	266	25.6	c.524G>A	p.Arg175His	SNV	Heterozygous
MEN131	<i>TP53</i>	chr17	7578413	346	63.3	c.517G>T	p.Val173Leu	SNV	Heterozygous
MEN134	<i>TP53</i>	chr17	7578478	148	77.0	c.452C>G	p.Pro151Arg	SNV	Heterozygous
MEN160	<i>TP53</i>	chr17	7579355	262	40.8	c.332T>A	p.Leu111Gln	SNV	Heterozygous
MEN169	<i>ARID1A</i>	chr1	27088742	113	61.9	c.2351G>A	p.Gly784Asp	SNV	Heterozygous
MEN169	<i>TP53</i>	chr17	7577076..7577077	704	69.6	c.861_862delGA	p.Glu287fs	Deletion	Heterozygous
MEN169	<i>CDKN2A</i>	chr9	21970984	216	59.7	c.374A>G	p.Asp125Gly	SNV	Heterozygous
MEN169	<i>CDKN2A</i>	chr9	21970987	215	60.5	c.371G>A	p.Arg124His	SNV	Heterozygous
MEN169	<i>CDKN2A</i>	chr9	21970990	183	56.8	c.368A>G	p.His123Gly	SNV	Heterozygous
MEN169	<i>CDKN2A</i>	chr9	21970991	183	56.8	c.367C>G	p.His123Gly	SNV	Heterozygous
MEN176	<i>TP53</i>	chr17	7578529	744	11.3	c.401T>C	p.Phe134Ser	SNV	Heterozygous
MEN192	<i>FLT3</i>	chr13	28592610	417	23.7	c.2535G>C	p.Arg845Ser	SNV	Heterozygous
MEN204	<i>TP53</i>	chr17	7578437	157	67.5	c.493C>T	p.Gln165*	SNV	Heterozygous
MEN208	<i>TP53</i>	chr17	7578394	169	81.7	c.536A>T	p.His179Leu	SNV	Heterozygous
KYSE30	<i>HRAS</i>	chr11	533874	719	70.1	c.182A>T	p.Gln61Leu	SNV	Heterozygous
KYSE30	<i>TP53</i>	chr17	7579358	332	24.1	c.329G>T	p.Arg110Leu	SNV	Heterozygous
KYSE30	<i>ASXL1</i>	chr20	31022641	904	32.2	c.2126C>T	p.Ala709Val	SNV	Heterozygous
KYSE30	<i>CDKN2A</i>	chr9	21971000	117	99.1	c.358G>T	p.Glu120*	SNV	Homozygous
KYSE50	<i>TP53</i>	chr17	7579386	334	100.0	c.301A>T	p.Lys101*	SNV	Homozygous
KYSE170	<i>TP53</i>	chr17	7577094	740	20.3	c.448C>G	p.Arg150Gly	SNV	Heterozygous
KYSE180	<i>HRAS</i>	chr11	534289	278	10.4	c.34G>A	p.Gly12Ser	SNV	Heterozygous
KYSE180	<i>TP53</i>	chr17	7578265	759	99.9	c.188T>C	p.Ile63Thr	SNV	Homozygous
KYSE220	<i>TP53</i>	chr17	7577539	563	98.0	c.346C>T	p.Arg116Trp	SNV	Homozygous
KYSE220	<i>CDKN2A</i>	chr9	21971153	179	98.3	c.205G>T	p.Glu69*	SNV	Homozygous
KYSE270	<i>EGFR</i>	chr7	55259524	1407	26.7	c.2582T>A	p.Leu861Gln	SNV	Heterozygous

